Catalysis Today 429 (2024) 114468

Contents lists available at ScienceDirect

Catalysis Today

journal homepage: www.elsevier.com/locate/cattod

Encapsulation of a bis-amino phenol precatalyst for the deoxydehydration of 1,2-hexanediol

Alixandre Magerat *, Sarah Eeckhout, Sophie Hermans, Eric M. Gaigneaux

Université catholique de Louvain, Institute of Condensed Matter and Nanosciences (IMCN) – Molecular Chemistry, Materials and Catalysis (MOST), Place Louis Pasteur, 1 – box 04.01.09, 1348 Louvain-la-Neuve, Belgium

ARTICLE INFO

Keywords:
Deoxydehydration
Encapsulation
SBA-1
Silylation
Rhenium

ABSTRACT

Nanoreactors encapsulating homogeneous catalysts behave as heterogeneous catalysts at the macroscopic scale, enabling the homogeneous catalyst to be easily recovered. One way to synthesize such nanoreactors is by inserting the homogeneous catalyst (or synthesizing it in situ) in the porosity of an inorganic oxide material, followed by a silylation reaction to narrow the pore entrance, preventing the outwards diffusion of the jailed homogeneous catalyst during the reaction. This way, the often-superior activity of homogeneous catalysts is combined with the robustness and the easy recovery of heterogeneous ones. Hereunder, we report for the first time the implementation of such a strategy towards the synthesis of a deoxydehydration (DODH) catalyst, namely a bis-amino phenol Re-complex. 1,2-hexanediol was used as the DODH vicinal diol model substrate. The encapsulation of the homogeneous catalyst in SBA-1 was demonstrated. It proved active in the DODH test reaction although not sustainably; the deactivation mechanism was therefore elucidated.

1. Introduction

The finiteness of oil resources and their ever-decreasing availability has pushed researchers to seek alternatives. Non-edible biomass is a promising substitute for petroleum-based chemicals, as it is abundant, renewable, and more easily accessible [1]. One of the main challenges in replacing petrochemicals is the polyoxygenated nature of biomolecules [2]. Hence, a prior deoxygenation is needed before being used in today's chemical industry. One of the ways – that has gained attention in recent years [3–5] – it can be achieved is deoxydehydration (DODH). DODH is a simultaneous dehydration and deoxygenation reaction occurring specifically on vicinal diols (Fig. 1a). This reaction, usually performed in the liquid phase, requires a sacrificial reductant and a high-valent metal-based (generally Re, Mo, or V) catalyst [6].

The main advantage of heterogeneous catalysts over homogeneous ones is their easy recyclability, which makes them more suitable for industrial implementation. This is why some researchers have spent time immobilizing soluble homogeneous catalysts onto insoluble supports. Homogeneous catalysts are generally immobilized through (1) covalent bonding [7], (2) adsorption (e.g. via electrostatic interactions) [8], or (3) physical entrapment [9,10]. Because of the molecular-like contact between the reactants and the dissolved catalyst, homogeneous catalysts often show superior catalytic performances than heterogeneous ones. The heterogenization of homogeneous catalysts without affecting their activity is thus a relevant strategy that must be explored. Among the above-mentioned strategies, physical entrapment is a particularly promising strategy as it allows the homogeneous catalyst to behave almost freely, as it does when it is free in solution, while making recovery possible.

Different encapsulation strategies exist such as the well-known ship-in-a-bottle (SIB) method [11], where the homogeneous catalyst is synthesized within the pores of a material. Quite recently, a modified SIB approach has been proposed to encapsulate homogeneous catalysts. In this approach, the homogeneous catalyst is instilled in the porosity of a material (or synthesized in situ), which is typically silica. The instillation is then followed by a silylation reaction in order to narrow the pore size, preventing the outwards diffusion of the jailed homogeneous catalyst (Fig. 2). To our knowledge, such a strategy has never been envisaged with DODH homogeneous catalysts. This is why we report hereunder the immobilization of one DODH homogeneous precatalyst, $L^4Re(CO)_3$, L^4 being 2-(((2-(dimethylamino)ethyl)(methyl)amino)methyl)phenol) [12,13] (Fig. 1b), by using the modified SIB approach. This precatalyst has been selected in the literature, inter alia, for its good catalytic performances under green conditions, its high thermal and air stability, its

* Corresponding author.
E-mail address: alixandre.magerat@uclouvain.be (A. Magerat).

https://doi.org/10.1016/j.cattod.2023.114468
Received 18 September 2023; Received in revised form 16 November 2023; Accepted 19 November 2023
Available online 23 November 2023

substrate versatility, and its ease of synthesis. For instance, this pre-catalyst, once activated in the presence of air, can convert erythritol to 1, 3-butadiene in the highest yields ever reported (78 %) [12]. SBA-1 was chosen as hosting material for its cage-like structure, its suitable textural properties, and its prior use in a similar application but for a different catalytic system including a Hoveyda-Grubbs catalyst for metathesis [14]. Other structured silica materials combined with other organometallic complexes have already been reported. For instance, SBA-16 has been used to encapsulate phophotungstic acid or molybdenum Schiff-bases for the epoxidation of olefins [9,15] and Fe(salen) for the production of optically active sulfoxides [10]. FDU-12 was used to host the Noyori catalyst for asymmetric hydrogenation [16]. Similarly SiO_2/Fe_2O_3 core/shell encapsulated n-heterocyclic carbene-gold(I) catalysts were prepared and used for alkyne hydration at low temperature (25 °C) [17].

2. Experimental section

2.1. Materials

D-fructose (≥99.5 %), dichloromethane (≥99.8 %), hydrochloric acid (37 % fuming) and sodium acetate (≥98.5 %) were purchased from Carl Roth. N,N,N′-trimethylethylenediamine (98 %) and sodium triacetoxyborohydride (97 %) were purchased from Fisher Scientific. 1,2-hexanediol (98 %), and bromopentacarbonylrhenium(I) (98 %) were purchased from Sigma-Aldrich. 1-bromohexadecane (>96 %), 1-hexene (>97.0 %), 3,5-di-tert-butyl-2-hydroxybenzaldehyde (>98.0 %), 3-octanol (>98.0 %), 3-octanone (>98.0 %), dichlorodiphenylsilane (>98.0 %), hexylmethyldichlorosilane (>95.0 %), n-octylmethyldichlorosilane (>97.0 %) and triethylamine (>99.0 %) were purchased from Tokyo Chemical Industry Europe.

2.2. Synthesis of $L^4Re(CO)3$ from Li et al. [12]

The $L^4Re(CO)_3$ complex was prepared following the procedure described by Li et al. [12]. Details are given in the supporting information. The compound was characterized by ^1H NMR, IR, and HRMS to confirm the success of the synthesis.

2.3. Synthesis of SBA-1 from Kao et al. [18]

The SBA-1 was prepared following the procedure described by Kao et al. [18]. Details are given in the supporting information. SBA-1 was characterized by pXRD and N_2 physisorption to confirm the success of the synthesis.

2.4. Encapsulation of $L^4Re(CO)_3$

In a round-bottom flask, 500 mg of SBA-1 was suspended in 25 mL of dichloromethane with 32 mg of $L^4Re(CO)_3$ to yield a 6 % $L^4Re(CO)_3$ wt. solid (nominal value). The suspension was stirred during 72 h and the solid was recovered by vacuum filtration and dried under reduced pressure overnight at room temperature. In order to reduce the pore entrance size, 100 mg of $L^4Re(CO)_3$/SBA-1 was suspended in a closed round-bottom flask with 5 mL n-hexane, namely a solvent in which $L^4Re(CO)_3$ is not soluble. Then, the silylating agent (3 mmol) was added and the mixture was stirred during 24 h at 35 °C. The solid was thoroughly washed with dichloromethane until disappearance of the phenyl UV-Vis signature in the supernatant. The same amount of dichloromethane was used to wash all the other silylated samples. Then the solid was recovered by filtration and dried overnight under vacuum. Samples silylated with dichlorodiphenylsilane (Ph), hexylmethyldichlorosilane (C_6) or n-octylmethyldichlorosilane (C_8) are denoted SBA-1(Y) where Y represents the grafted functional group (Ph, C_6 or C_8).

2.5. Catalytic tests

To a 35 mL closed pressure tube (Ace) equipped with a PTFE stirrer, 5 mL of a 3-octanol solution containing 0.5 mmol of 1,2-hexanediol and 0.5 mmol dodecane (internal standard) are added together with 100 mg (pre)catalyst when supported or 6 mg of pure $L^4Re(CO)_3$. The reaction was performed at 180 °C (oil bath temperature) during 24 h. Afterwards, the tube was cooled down in an ice-cold water bath. Reactants and products were quantified with a GC-2010 Plus equipped with a FID-2010 Plus detector, a SH-RTX-5 (30 m length, 0.25 mm inner diameter, 0.1 μm film thickness) column, an AOC-20 s auto-sampler, and an AOC-20i auto-injector from Shimadzu. An aliquot of 1 μL of the prepared vial was injected (injector temperature: 275 °C, 70 °C during 6 min and then 20 °C/min until 100 °C) and the analysis was performed in split mode (split = 15, inlet pressure = 25 psi).

2.6. Leaching tests

Since the catalyst absorbs in UV–vis, to test whether leaching was occurring during the reaction, an aliquot of the supernatant of the reaction mixture was diluted in 3-octanol in a quartz High Precision Cell from Hellma Analytics (10 mm length path) for analysis. The spectrum (230–400 nm) was recorded on a Shimadzu UV-3600 Plus Series spectrometer.

2.7. Characterization of the samples

2.7.1. Fourier-transform infrared spectroscopy (FTIR)

Powders were diluted in dry KBr and pressed in self-supporting wafers. FTIR spectra were recorded on a Bruker Equinox 55 equipped with a dielectric DTGS detector with an iris aperture of 5000 μm. A pure KBr wafer was recorded and used as background. One hundred scans were carried out in the range of 400–4000 cm^{-1} in order to yield a 4 cm^{-1} resolution.

2.7.2. UV–vis spectroscopy

Solutions were analyzed in a Shimadzu UV-3600 Plus Series spectrometer in quartz High Precision Cells from Hellma Analytics. The spectra were recorded from 200 nm to 800 nm with a 0.5 nm sampling interval (slit width of 2 nm). From 200–380 nm, a deuterium lamp from Shimadzu was used as source while a W-lamp halogen was used as source for the rest of the spectrum.

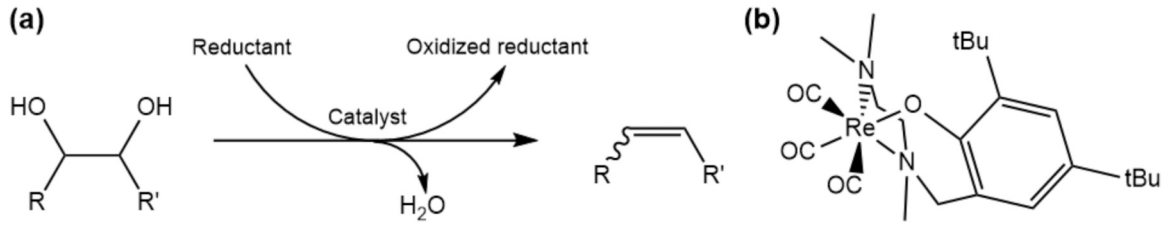

Fig. 1. (a) Deoxydehydration of a vicinal diol. (b) Bis-amino-phenol rhenium precatalyst $L^4Re(CO)_3$, L^4 being 2-(((2-(dimethylamino)ethyl)(methyl)amino) methyl)phenol).

2.7.3. Powder X-ray Diffraction (pXRD)

Diffractograms of the samples were recorded on a Bruker-D8 Advance diffractometer with a Bragg-Brentano geometry. A copper anode operated under 40 kV (Kα = 0.154 nm) and 30 mA was used as X-ray source. The detector was a LynxEye XE-T. The angle (2Θ) was varied from 5° to 80° at a speed of 5.93°/min (5051 steps of 0.015°). Well grinded powders were dispersed on a "zero noise" sample holder coated with Nivea cream before insertion in the apparatus.

2.7.4. N_2 physisorption

The textural properties of powders were quantified thanks to N_2 physisorption. The Brunauer-Emmett-Teller (BET) model was applied to assess the specific surface area using partial pressures out of the [0.05–0.3] range. As the Barrett-Jowner-Halenda (BJH) model is not suitable for micropores, a density functional theory (DFT) provided by Micromeritics was applied (N_2, cylindrical pores, oxide surface) to evaluate pore size distribution. The pore diameter reported hereunder refers to the maximum observed in the pore diameter distribution. Samples were weighed before and after degassing overnight with a Micromeritics VacPrep061 machine at 150–200 °C and at about 50 mTorr. Nitrogen physisorption measurements were carried out using a liquid N_2 bath with a Micromeritics 3Flex apparatus.

2.7.5. X-ray photoelectron spectroscopy (XPS)

The analyses were carried out with a SSX 100/206 photoelectron spectrometer from Surface Science Instruments (USA) equipped with a monochromatized micro focused Al X-ray source (powered at 20 mA and 10 kV). The sample powders pressed in small stainless-steel troughs of 4 mm diameter were placed on a ceramic carousel. The pressure in the analysis chamber was around 10^{-6} Pa. The angle between the surface normal and the axis of the analyser lens was 55°. The analyzed area was approximately 1.4 mm^2 and the pass energy was set at 150 eV. In these conditions, the full width measured at half maximum (FWHM) of the Au $4f_{7/2}$ peak for a clean gold standard sample was about 1.6 eV. A flood gun set at 8 eV and a Ni grid placed above the sample surface were used for charge stabilization. The following sequence of spectra was recorded: survey spectrum, C 1s, O 1s, N 1s, Cl 2p, Re 4f for samples containing Re and C 1s again to check the stability of charge compensation with time. The aromatic C-(C,H) component of the C1s peak of carbon was fixed to 284.8 eV to set the binding energy scale. Data treatment was performed with the CasaXPS program (Casa Software Ltd, UK). Some spectra were decomposed with the least squares fitting routine provided by the software with a Gaussian/Lorentzian (85/15) product function and after subtraction of a non-linear baseline. Molar fractions were calculated using peak areas normalized based on acquisition parameters and sensitivity factors provided by the manufacturer.

2.7.6. Inductively coupled plasma-atomic emission spectroscopy

The rhenium load in each composite solid was measured by ICP-AES. For this matter, 50 mg of each sample was mixed with 1 g of NaOH and Na_2O_2 and melted on the flame of a Bunsen burner. Melted samples were acidified with HCl and diluted with distilled water prior to analysis.

3. Results and discussion

SBA-1 [18] and $L^4Re(CO)_3$ [12] were synthesized according to the literature. The presence of 3 reflection peaks (2θ = 2.15°, 2.38° and 2.60°) characteristic of the $Pm\bar{3}n$ symmetry corresponding to the planes (200), (210) and (211) (Fig. 3, right) as well as the expected textural properties (specific surface area between 1200 m^2/g and 1450 m^2/g and pore diameter between 2 and 3 nm) (Table 1) confirm the correct synthesis of SBA-1 [19]. The success of the synthesis of highly pure $L^4Re(CO)_3$ is also confirmed by ^1H NMR, FTIR and High Resolution Mass Spectrometry (Supporting Information).

After encapsulation, the IR spectrum of $L^4Re(CO)_3$/SBA-1(Y) was first recorded to verify whether the silylation occurred successfully (Fig. 3, left). The C-H bands around 3000 cm^{-1} for $L^4Re(CO)_3$/SBA-1(C_8 or C_6) and the bands of aromatic ring vibration at 1429 cm^{-1} show the presence of alkanes. The Si-Ph stretching peak (1127 cm^{-1}), the bands of aromatic ring vibration at 1429 cm^{-1} and the C-H vibration peaks of aromatics at 720, 737 and 698 cm^{-1} indicate the presence of phenyl groups (Ph) after silylation of SBA-1. Moreover, the decreasing specific surface area, pore diameter and pore volume are consistent with a correct functionalization. Textural properties with and without $L^4Re(CO)_3$ were identical due to the low $L^4Re(CO)_3$ loading. The fact that the phenyl or alkyl functional groups are really covalently anchored to the SBA-1 surface is supported by the presence of IR-visible phenyl groups on the SBA-1 surface after thoroughly washing with dichloromethane the SBA-1(Ph) sample until disappearance of its UV–vis signature. As the C_6 and C_8-silylated SBA-1 were washed the same way, it is assumed that alkyl groups are also covalently linked.

pXRD was performed on SBA-1(Y) to ensure that HCl – produced as byproduct during the silylation – was not deteriorating the cage-like structure of SBA-1. None of the silylated powders presented a different structure than pristine SBA-1 (cubic structure with Pm3n symmetry, Fig. 3).

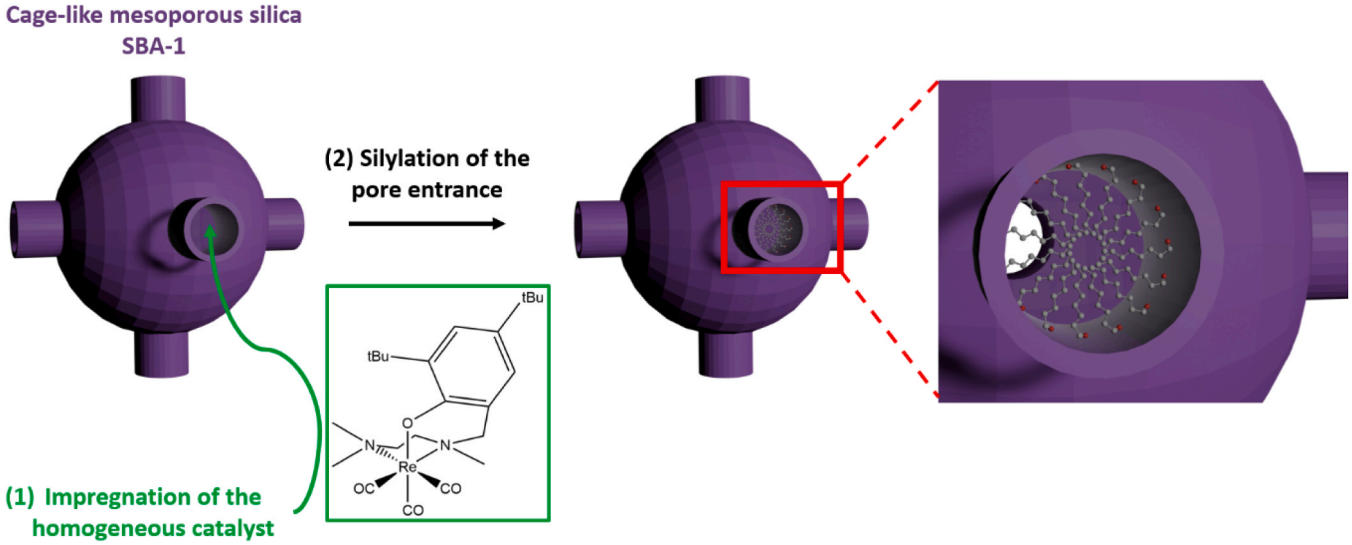

Fig. 2. Strategy of immobilization. (1) Instillation of $L^4Re(CO)_3$ followed by (2) Pore size narrowing through silylation. This scheme is used for illustration only.

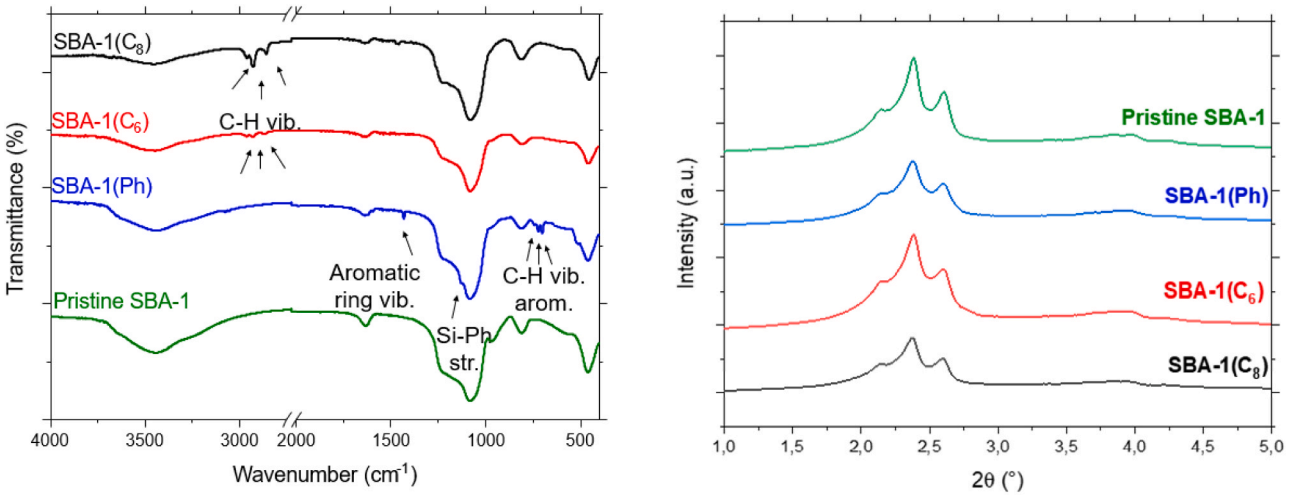

Fig. 3. FTIR spectra (left) and pXRD diffractograms of silylated $L^4Re(CO)_3$/SBA-1(Y).

Table 1
Textural properties of pristine SBA-1 and silylated SBA-1.

Sample	S_{BET} (m^2/g)	Micro. Vol. (cm^3/g STP)	Pore diameter (Å)
SBA-1	1254	186	20
SBA-1(Ph)	320	76	10
SBA-1(C_6)	300	71	11
SBA-1(C_8)	417	92	15

XPS and ICP-AES analyses were performed to decipher whether $L^4Re(CO)_3$ was intact and located inside or at the external surface of SBA-1. No Re nor N (elements that could only come from $L^4Re(CO)_3$) was detected by XPS while Re was detected by ICP-AES (see data given in the Supporting information). This confirmed that the precatalyst was inside the silylated SBA-1. Additionally, a thoroughly washed $L^4Re(CO)_3$/SBA-1(Ph) solid was stirred during 24 h in 3-octanol at 180 °C. Then, the supernatant was analyzed by UV–vis without dilution to see whether the catalyst had leached or not under these conditions. A tiny – in comparison to what was observed in the presence of water – peak at 270 nm was observed (absorbance = 0.015, Supporting Information). However, this can be explained by the traces of water produced by the slight dehydration reaction of 3-octanol that could occur during this experiment [12]. As was reported in the literature, $L^4Re(CO)_3$ indeed proved to be a DODH-active catalyst for 1,2-hexanediol transformation (Fig. 4). Recycling tests were then performed to test the stability of the heterogenized $L^4Re(CO)_3$ precatalyst. Upon recycling, the 1-hexene yield dramatically decreased (Fig. 5). Supernatants of these catalytic tests were recovered and their UV–vis spectra were compared to the one of $L^4Re(CO)_3$ before and after catalytic test. All supernatants showed a spectrum with a peak at 270 nm, characteristic of $L^4Re(CO)_3$ once activated (Fig. 6). This evidences the occurrence of leaching of the catalyst during the catalytic test. Moreover, three peaks at 260, 266 and 272 nm were observed only in the UV–vis spectrum of $L^4Re(CO)_3$/SBA-1(Ph). These peaks are characteristic of the chromophore part of dichlorodiphenylsilane (see UV–vis spectrum of dichlorodiphenylsilane in the Supporting Information), namely the silylating agent used for this sample. This means that this molecule is leaching from the SBA-1 surface into the solution during the catalytic tests. The cause of this leaching was investigated, as it could prompt, in turn, the leaching of the encapsulated catalyst.

In literature, some researchers have already reported on ≡Si-OR instability, mainly its inherent hydrolyzability [20]. For instance, Bui et al. reported the hydrolysis of siloxane by water at 130 °C [21]. Additionally, polar molecules have been found to provoke leaching, especially at high temperatures [22]. However, the conditions under which leaching was observed are case-dependent and no clear tendency has been pointed out yet.

As DODH inescapably produces water, experiments were carried out to see whether the leaching of phenyl group moieties – the only silylating agent visible through UV–vis spectroscopy –was caused by the presence of water. Thus, 100 mg of extensively washed SBA-1(Ph) was suspended in 3-octanol (5 mL) in the presence and in the absence of water (10 μL) under the same conditions as used in the catalytic tests. The suspension was then filtered and the supernatant was analyzed by UV–vis spectrometry. In the presence of water, the three above-mentioned peaks that are typical of the silylating agent appeared while it was not the case in the experiment carried out without water (Fig. 7, left). This evidences that leaching was caused because of the presence of water, which by gate-opening provoked the escape of the active complex. The hydrolysis chemistry was not investigated as it is still matter of debate but the SiOR bond is believed to be cleaved. In order to minimize leaching of the grafted functional groups, the temperature of the catalytic test was thereupon decreased to 120 °C, temperature at which the activity of the free precatalyst is low (Fig. 7, right). However, the leaching of phenyl moieties was still observed (Fig. 7, left). Assuming that other silylating agents (C_6 and C_8) undergo the same behavior than dichlorodiphenylsilane, we concluded that the modified ship-in-the-bottle (SIB) strategy was not compatible for this catalytic

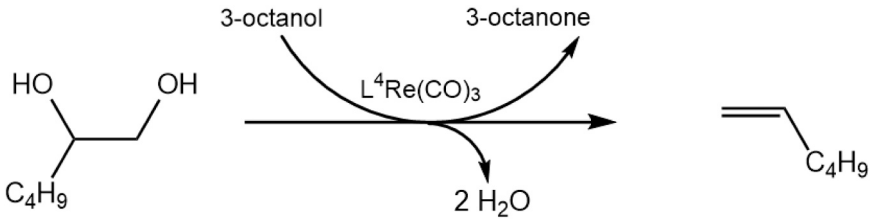

Fig. 4. DODH model reaction studied in this contribution.

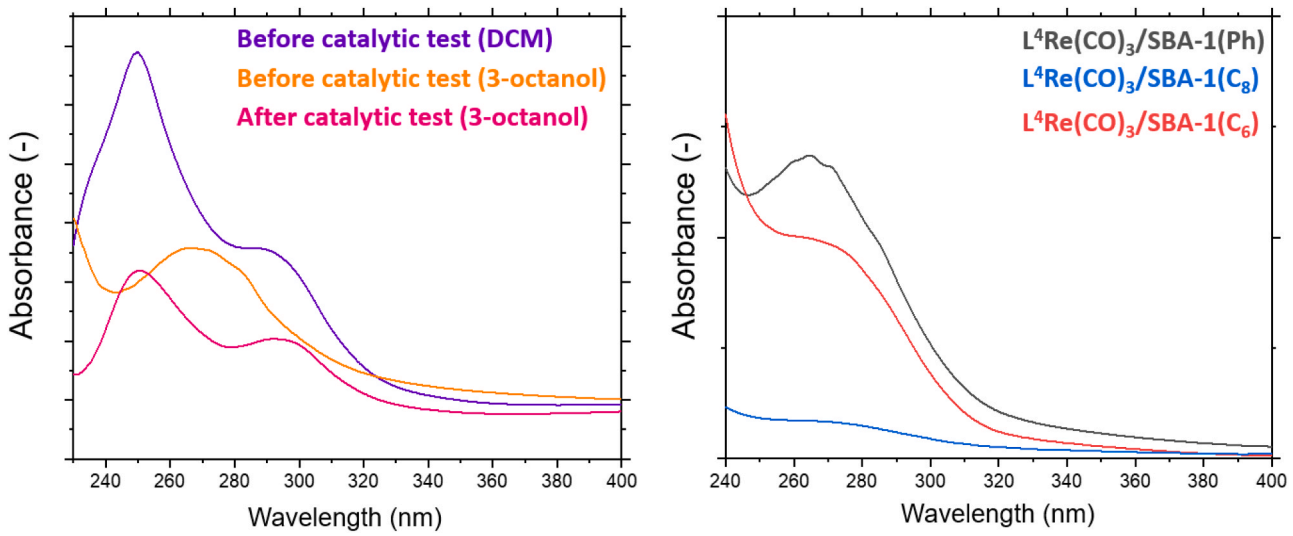

Fig. 5. LEFT. UV–vis spectra of the precatalyst in dichloromethane (purple), and 3-octanol (yellow) and the catalyst in 3-octanol after test (pink). RIGHT. UV–vis spectra of the supernatants of the reaction medium after catalytic tests with different solids.

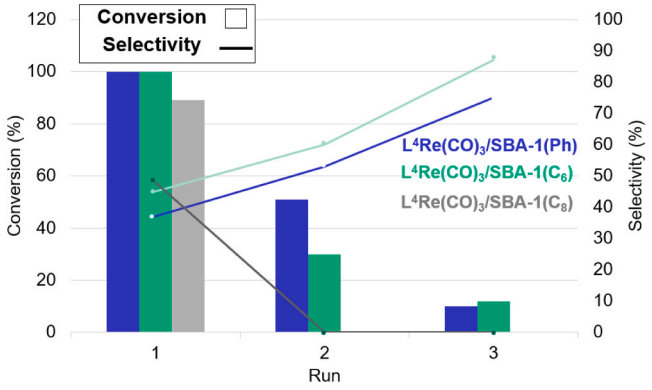

Fig. 6. Catalytic performances of the $L^4Re(CO)_3$/SBA-1(Y) systems. Reaction conditions: 5 mL of 3-octanol containing 1,2-hexanediol (0.1 mol/L) and dodecane (0.1 mol/L) as internal standard. 180 °C, 24 h and 100 mg of solid.

system, and likely all other reactions producing water as a byproduct and requiring high temperatures. Other strategies must therefore be envisaged in the future. For instance, the ligands of this type of catalyst could be modified – without modifying the catalytic performances – inside the porosity of SBA-1, after instillation, by using more bulky ligands (classical SIB method). A desiccant could also be added to the catalytic reaction medium to prevent hydrolysis within the solid catalyst, but it should not interfere negatively with the reaction. Lastly, one could increase the hydrophobicity of the silylating agents to prevent their hydrolysis at the silica surface, or as a general idea increase the robustness of the bonds between silica and pore-blocking agents.

4. Conclusion

To summarize, we managed to demonstrate why the strategy of narrowing the pores by silylation after instillation of a homogeneous catalyst is not compatible with the catalytic conditions required to perform DODHs. Indeed, the functionalization used to enjail $L^4Re(CO)_3$ in the porosity of the SBA support is degrafted in the presence of water, an unavoidable by-product in DODH. As a consequence, $L^4Re(CO)_3$ becomes free to escape the pores of the support during the catalytic tests, thereby performing its catalytic effect in the homogenous phase, but is not recovered in the recycled solids. Nevertheless, our work demonstrated that the complex was successfully entrapped, meaning heterogenized and processable as a solid, thanks to our instillation-silylation strategy. Our strategy and catalysts are therefore much more likely to be efficient in other reactions than DODH where anhydrous conditions can

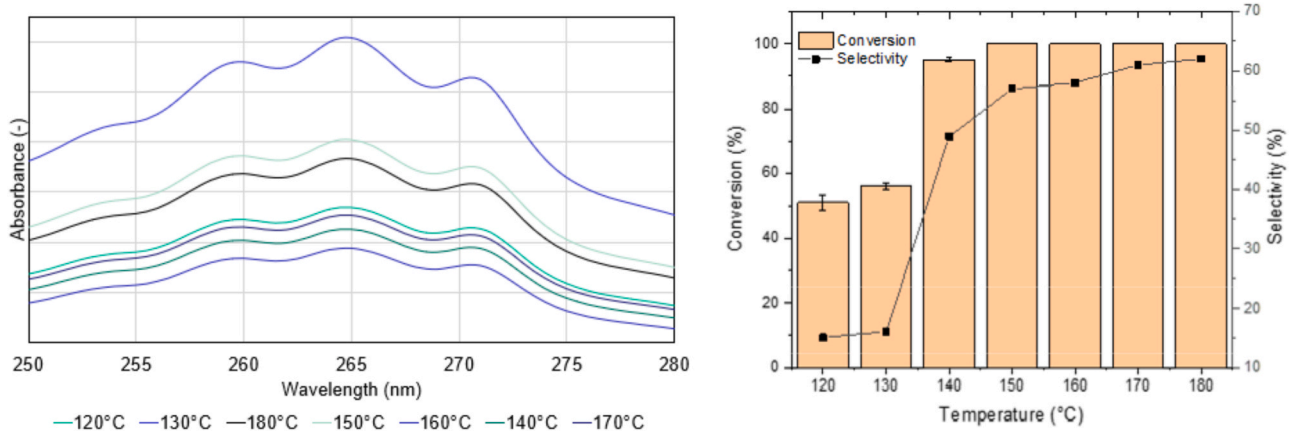

Fig. 7. LEFT. UV–vis spectra of the supernatants obtained by mixing 100 mg SBA-1(Ph), 5 mL 3-octanol and 10 µL water at different temperatures. RIGHT. Catalytic performances of the free $L^4Re(CO)_3$.

be maintained.

CRediT authorship contribution statement

Alixandre Magerat: Conceptualization, Methodology, Formal analysis, Writing – original draft, Investigation. **Sarah Eeckhout:** Methodology, Conceptualization. **Eric M. Gaigneaux:** Project administration, Validation, Writing – review & editing. **Sophie Hermans:** Project administration, Validation, Writing – review & editing.

Declaration of Competing Interest

The authors declare that they have no known competing financial interests or personal relationships that could have appeared to influence the work reported in this paper.

Data availability

Data will be made available on request.

Acknowledgements

The first author thanks the Université catholique de Louvain (UCLouvain) for the teaching assistant position as well as the organising committee of the PREPA13 (13th Symposium on the Scientific Bases for the Preparation of Heterogeneous Catalysts) for giving him the opportunity to contribute to this special issue in Catalysis Today. Many thanks to Michaël Scarito for the silylation scheme and to the lab technicians that have aided in the analysis of our samples.

Appendix A. Supporting information

Supplementary data associated with this article can be found in the online version at doi:10.1016/j.cattod.2023.114468.

References

[1] J.R. Dethlefsen, P. Fristrup, Rhenium-catalyzed deoxydehydration of diols and polyols, ChemSusChem 8 (5) (2015) 767–775, https://doi.org/10.1002/cssc.201402987.
[2] C. Boucher-Jacobs, K.M. Nicholas, Deoxydehydration of polyols, in: K.M. Nicholas (Ed.), Selective Catalysis for Renewable Feedstocks and Chemicals, Springer International Publishing, Cham, 2014, pp. 163–184, https://doi.org/10.1007/128_2014_537.
[3] K. Yamaguchi, J. Cao, M. Betchaku, Y. Nakagawa, M. Tamura, A. Nakayama, M. Yabushita, K. Tomishige, Deoxydehydration of biomass-derived polyols over silver-modified ceria-supported rhenium catalyst with molecular hydrogen, ChemSusChem 15 (10) (2022), e202102663, https://doi.org/10.1002/cssc.202102663.
[4] N.N. Tshibalonza, J.-C.M. Monbaliu, The deoxydehydration (DODH) reaction: a versatile technology for accessing olefins from bio-based polyols, Green. Chem. 22 (15) (2020) 4801–4848, https://doi.org/10.1039/D0GC00689K.
[5] J. Sebastian, C. Mebrahtu, R. Palkovits, Influence and stability of the surface density of MoO_x on TiO_2 in deoxydehydration: structure–activity correlations, Catal. Sci. Technol. 13 (4) (2023) 1087–1097, https://doi.org/10.1039/D2CY01854C.
[6] F.C. Jentoft, Transition metal-catalyzed deoxydehydration: missing pieces of the puzzle, Catal. Sci. Technol. (2022), https://doi.org/10.1039/D1CY02083H.
[7] C. Vriamont, M. Devillers, O. Riant, S. Hermans, A covalently anchored homogeneous gold complex on carbon nanotubes: a reusable catalyst, Chem. Commun. 49 (89) (2013) 10504–10506, https://doi.org/10.1039/C3CC46097E.
[8] H. Yang, Z. Ma, Y. Wang, Y. Wang, L. Fang, Hoveyda–Grubbs catalyst confined in the nanocages of SBA-1: enhanced recyclability for olefin metathesis, Chem. Commun. 46 (45) (2010) 8659–8661, https://doi.org/10.1039/C0CC03227A.
[9] M. Masteri-Farahani, M. Modarres, Encapsulation of Keggin-Type phosphotungstic acid into the mesopores of SBA-16 as a reusable heterogeneous catalyst for the epoxidation of olefins, Sci. Iran. 24 (6) (2017) 2993–3001, https://doi.org/10.24200/sci.2017.4492.
[10] R.L. Oliveira, T. Nijholt, M. Shakeri, P.E. de Jongh, R.J.M.K. Gebbink, K.P. de Jong, Encapsulation of chiral Fe(Salen) in mesoporous silica structures for use as catalysts to produce optically active sulfoxides, Catal. Sci. Technol. 6 (13) (2016) 5124–5133, https://doi.org/10.1039/C6CY00113K.
[11] E. Páez-Mozo, N. Gabriunas, R. Maggi, D. Acosta, P. Ruiz, B. Delmon, Selective olefin oxidation with cobalt phthalocyanine encapsulated in Y-zeolite, J. Mol. Catal. 91 (2) (1994) 251–258, https://doi.org/10.1016/0304-5102(94)00027-1.
[12] J. Li, M. Lutz, R.J.M. Klein Gebbink, N,N,O-coordinated tricarbonylrhenium precatalysts for the aerobic deoxydehydration of diols and polyols, Catal. Sci. Technol. 10 (11) (2020) 3782–3788, https://doi.org/10.1039/D0CY00618A.
[13] J. Li, Molecular Rhenium and Molybdenum-based (pre)catalysts for the deoxydehydration of vicinal diols and biomass-derived polyols. URN:NBN:NL:UI:10-1874-397381, Utrecht University,, 2020. ⟨https://dspace.library.uu.nl/bitstream/handle/1874/397381/5ee36a8a1b05cLi.pdf?sequence=1⟩.
[14] H. Yang, Z. Ma, T. Zhou, W. Zhang, J. Chao, Y. Qin, Encapsulation of an olefin metathesis catalyst in the nanocages of SBA-1: facile preparation, high encapsulation efficiency, and high activity, ChemCatChem 5 (8) (2013) 2278–2287, https://doi.org/10.1002/cctc.201300021.
[15] M. Masteri-Farahani, M.-S. Hosseini, Z. Miri, Encapsulation of molybdenum schiff-base complex inside the SBA-16 nanocages with ship-in-a–bottle strategy for selective epoxidation of alkenes, ChemistrySelect 6 (45) (2021) 12582–12589, https://doi.org/10.1002/slct.202103106.
[16] J. Peng, X. Wang, X. Zhang, S. Bai, Y. Zhao, C. Li, Q. Yang, Asymmetric hydrogenation by RuCl2(R-Binap)(Dmf)n encapsulated in silica-based nanoreactors, Catal. Sci. Technol. 5 (2) (2015) 666–672, https://doi.org/10.1039/C4CY00228H.
[17] B.Ö. Öztürk, B. Çetinel, S. Karabulut Şehitoğlu, Encapsulation of N-heterocyclic carbene–gold (i) catalysts within magnetic core/shell silica gels: a reusable alkyne hydration catalyst, Appl. Organomet. Chem. 34 (9) (2020), e5686, https://doi.org/10.1002/aoc.5686.
[18] H.-M. Kao, C.-C. Ting, A.S.T. Chiang, C.-C. Teng, C.-H. Chen, Facile synthesis of stable cubic mesoporous silica SBA-1 over a broad temperature range with the aid of d-fructose, Chem. Commun. (No. 8) (2005) 1058–1060, https://doi.org/10.1039/B414786C.
[19] S. Jarmolińska, A. Feliczak-Guzik, I. Nowak, Synthesis, characterization and use of mesoporous silicas of the following types SBA-1, SBA-2, HMM-1 and HMM-2, Materials 13 (19) (2020) 4385, https://doi.org/10.3390/ma13194385.
[20] G.C. Ossenkamp, T. Kemmitt, J.H. Johnston, New approaches to surface-alkoxylated silica with increased hydrolytic stability, Chem. Mater. 13 (11) (2001) 3975–3980, https://doi.org/10.1021/cm000883t.
[21] T.V. Bui, S.J. Umbarila, B. Wang, T. Sooknoi, G. Li, B. Chen, D.E. Resasco, High-temperature grafting silylation for minimizing leaching of acid functionality from hydrophobic mesoporous silicas used as catalysts in the liquid phase, Langmuir 35 (21) (2019) 6838–6852, https://doi.org/10.1021/acs.langmuir.9b00487.
[22] A.C. Alba-Rubio, F. Vila, D.M. Alonso, M. Ojeda, R. Mariscal, M. López Granados, Deactivation of organosulfonic acid functionalized silica catalysts during biodiesel synthesis, Appl. Catal. B: Environ. 95 (3) (2010) 279–287, https://doi.org/10.1016/j.apcatb.2010.01.005.